Article

Theory of the Vom Berg Rheological Model and Its Use in Cloud-Native Application

Rafał Wiśniowski (ID) **and Grzegorz Orłowicz** *(ID)

Faculty of Drilling Oil and Gas, Department of Drilling and Geoengineering, AGH University of Science and Technology, 30 Mickiewicza Av., 30-059 Kraków, Poland; wisnios@agh.edu.pl
* Correspondence: orlowiczg@gmail.com; Tel.: +48-517-693-870

Abstract: Various technological fluids, such as drilling muds, drill-in fluids, fracturing fluids, spacers, washes and cement slurries are used in the wellbore drilling process. The fundamental issue, which needs to be addressed in order to become acquainted with the phenomena occurring during fluids flow through a circulatory system, is to establish mutual dependencies between a stream of fluid being pumped and flow resistances. The awareness of these dependencies enables the optimisation of hydraulic parameters in order to minimise costs and maximise drilling works safety. This article presents rheological models of drilling fluids and proposes the application of a new rheological model, not used in the drilling industry so far, namely the Vom Berg model. The model has been presented in other publications; however, there is an unsolved and unpublished problem of determining the effect of rheological parameters of the model on the value of resistance to laminar and turbulent flow. In this article, algorithms and Cloud-Native application enabling numerical determination of rheological properties of the Vom Berg fluid are presented. What is more, an algorithm for calculating pressure losses during the laminar flow of fluid in a pipe is provided. Taking an example from the industry, a practical application of the proposed calculation methodology is presented.

Keywords: drilling; drilling fluids; rheology; rheological model; numerical methods

1. Introduction

A number of boreholes are made every year for the needs of the energy and environmental engineering sectors. When drilling oil wells and geothermal boreholes, it is possible to acquire fluid energy raw materials and store energy and, when using trenchless technologies (horizontal directional drilling, microtunneling direct pipe), the underground transport of utilities to long distances is ensured. During making boreholes, various technological fluids are used, such as drilling muds, drill-in fluids, fracturing fluids, spacers, washes and cement slurries. The knowledge of physicochemical phenomena occurring during drilling fluid flow enables rational designing of the technique and technology in order to guarantee maximum works safety and minimum investment expenditures.

The fundamental issue, which needs to be solved in order to learn about the phenomena occurring during drilling fluids flow through a circulatory system, is to establish mutual dependencies between a stream of fluid being pumped and flow resistances occurring when it is pumped.

Flow resistances in any circulatory system component depend on the following:

- The type of flowing fluid;
- Geometry and physical properties of the element in which flow takes place;
- Flow regime.

The most important factors affecting the amount of pressure losses include physical properties and rheological parameters of the flowing fluid.

This article presents rheological models of drilling fluids and proposes the application of a new rheological model, not used in the drilling industry so far, namely the Vom Berg

model. The model has been presented in other publications [1,2]; however, there is an unsolved and unpublished problem of determining the effect of rheological parameters of the model on the value of resistance to laminar and turbulent flow. The aim of this study was to present in detail the laminar flow of fluid described by the Vom Berg model.

2. Division of Drilling Fluids According to Rheological Properties

In most cases, fluids used in the drilling industry are Newtonian fluids, viscoplastic (Bingham plastics) and pseudoplastic (Ostwald de Waele).

An API RP 13D (American Petroleum Institute Recommended Practice 13D) standard, containing recommendations concerning rheological studies and hydraulic calculations of drilling fluids, recommends using one of the three models: Bingham, Ostwald de Waele (power law) or Herschel–Bulkley (yield power law) [3–6]. The form of models are presented in Equations (1)–(3):

- Bingham model:

$$\tau = \tau_y + \eta \cdot \left(-\frac{dv}{dr} \right) \tag{1}$$

- Ostwald de Waele model (power law):

$$\tau = k \cdot \left(-\frac{dv}{dr} \right)^n \tag{2}$$

- Herschel–Bulkley model (yield power law):

$$\tau = \tau_y + k \cdot \left(-\frac{dv}{dr} \right)^n \tag{3}$$

The application of chemical agents enabling the modification of physical properties and rheological parameters of drilling muds and cement slurries causes those fluids to potentially demonstrate both the features of viscoelastic fluids and pseudoplastic fluids.

Thus, for this kind of fluid, other rheological models should be considered. One of the possible ones is the Vom Berg model in the form of [1,2,7]:

$$\tau = \tau_y + D \cdot \sinh^{-1} \left(\frac{-\frac{dv}{dr}}{G} \right) \tag{4}$$

3. Laminar Flow of Reostable Fluids through a Pipe

Finding dependencies between a stream of flowing fluid and flow resistances is possible after considering fluid flow in a straight horizontal pipe. From the stream of fluid, we can distinguish (Figure 1) a part of fluid volume in the form of a cylinder with the radius r and the length of ΔL.

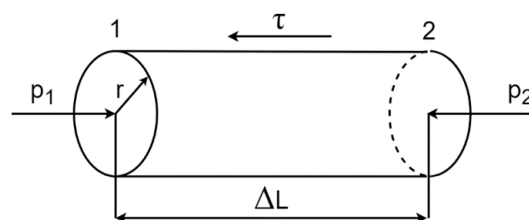**Figure 1.** Distribution of stresses during laminar flow of fluid through a pipe.

In order to obtain the condition of balance of forces applied at separate mass of fluids, the sum of projections of external forces on the direction of the pipe axis has to equal zero.

Assuming that flow occurs to the right $p_1 > p_2$, the forces distribution is as follows:

- Pressure $p_1 = p$ acts on cross Section 1 with an area of πr^2,

- Pressure p_2 acts on cross Section 2 with an area of πr^2, that pressure by number equals to pressure p reduced by pressure losses at the length ΔL: $p_2 = \left(p - \frac{dp}{dl}\Delta l\right)$,
- At the cylinder side with an area of $2\pi r\Delta l$ friction force occurs during flow, which is caused by shear stresses τ coming from the fluid.

The equilibrium equation of forces can be thus written in the form of

$$p\pi r^2 - 2\pi r\Delta l\tau - \left(p - \frac{dp}{dl}\Delta l\right)\pi r^2 = 0 \tag{5}$$

After transformation, we receive:

$$\frac{dp}{dl} = \frac{2}{r}\tau \tag{6}$$

The above equation is a basic dependency enabling the establishment of correlations between a stream of fluid flowing through a pipe (regardless of its rheological properties) and flow resistances in the laminar regime.

The sought relationships for the Vom Berg model can be obtained by inserting to Equation (6) rheological Equation (4):

$$\frac{dp}{dl} = \frac{2}{r}\left(\tau_y + D \cdot \sinh^{-1}\left(\frac{-\frac{dv}{dr}}{G}\right)\right) \tag{7}$$

From Equation (7), one can determine a shear rate gradient $\dot{\gamma} = \left(-\frac{dv}{dr}\right)$ by means of the following relationship:

$$\left(-\frac{dv}{dr}\right) = G\sinh\left(\frac{r}{2D}\frac{dp}{dl} - \frac{\tau_y}{D}\right) \tag{8}$$

After variables separation in Equation (8) and integration, the following is obtained:

$$v = -G\frac{2D}{\frac{dp}{dl}}\cosh\left(\frac{r}{2D}\frac{dp}{dl} - \frac{\tau_y}{D}\right) + C_1 \tag{9}$$

The constant C_1 is determined from the boundary conditions. It is assumed that at the pipe wall, for the value r = R, the fluid stream flow rate is v = 0.

$$C_1 = G\frac{2D}{\frac{dp}{dl}}\cosh\left(\frac{R}{2D}\frac{dp}{dl} - \frac{\tau_y}{D}\right) \tag{10}$$

By inserting the value C_1 to Equation (9), we obtain the distribution of the Vom Berg fluid flow rate along the radius of the pipe in which flow takes place:

$$v = G\frac{2D}{\frac{dp}{dl}}\left[\cosh\left(\frac{R}{2D}\frac{dp}{dl} - \frac{\tau_y}{D}\right) - \cosh\left(\frac{r}{2D}\frac{dp}{dl} - \frac{\tau_y}{D}\right)\right] \tag{11}$$

The minimum speed value is zero and occurs at the pipe wall. The maximum fluid flow rate is determined from the following condition: $v'(r_0) = 0 \wedge v''(r_0) < 0$. This rate occurs at a distance $r_0 = \frac{2\tau_y dl}{dp}$ from the pipe centre and is determined on the basis of the following formula:

$$V_{max} = G\frac{2D}{\frac{dp}{dl}}\left[\cosh\left(\frac{R}{2D}\frac{dp}{dl} - \frac{\tau_y}{D}\right) - 1\right] \tag{12}$$

The total stream of the Vom Berg fluid is the sum of the fluid nucleus stream Q_0 (a cylinder with the radius r_0 moving with constant velocity $v_0 = v_{max}$) and stream Q_1 flowing around a hollow cylinder with the internal radius r_0 and the external radius R.

$$Q = \int_0^R v(r)dF = \int_0^{r_0} v_0 dF + \int_{r_0}^R v(r)dF \tag{13}$$

Assuming unit cross-section dF = $2\pi r dr$, the total stream of the Vom Berg fluid flowing through a pipe is determined on the basis of the following dependence:

$$Q = Q_0 + Q_1 = v_0 \pi r_0^2 + \int_{r_0}^R v(r)dF \tag{14}$$

$$Q = v_0 \pi r_0^2 + \int_{r_0}^R G \frac{2D}{\frac{dp}{dl}} \left[\cosh\left(\frac{R}{2D}\frac{dp}{dl} - \frac{\tau_y}{D} \right) - \cosh\left(\frac{r}{2D}\frac{dp}{dl} - \frac{\tau_y}{D} \right) \right] 2\pi r dr \tag{15}$$

By determining the integral in Equation (15) and taking into account the relationship $r_0 = \frac{2\tau_y dl}{dp}$, we obtain:

$$Q = \frac{16\pi GD^3}{\left(\frac{dp}{dl} \right)^3} \left[\left(\frac{R^2}{8D^2} \left(\frac{dp}{dl} \right)^2 + 1 \right) \cosh\left(\frac{R}{2D}\frac{dp}{dl} - \frac{\tau_y}{D} \right) - \frac{R}{2D}\frac{dp}{dl}\sinh\left(\frac{R}{2D}\frac{dp}{dl} - \frac{\tau_y}{D} \right) - \frac{(\tau_y)^2}{2D^2} - 1 \right] \tag{16}$$

The dependence of unit pressure losses $\left(\frac{dp}{dl} \right)$ on the flow stream for laminar flow (Q) of the Vom Berg fluid is determined by means of the implicit function theorem (16).

In order to solve Equation (16), the following function is created:

$$g(x) = \frac{16\pi GD^3}{(x)^3} \left[\left(\frac{R^2}{8D^2}(x)^2 + 1 \right) \cosh\left(\frac{R}{2D}x - \frac{\tau_y}{D} \right) - \frac{R}{2D}x\sinh\left(\frac{R}{2D}x - \frac{\tau_y}{D} \right) - \frac{(\tau_y)^2}{2D^2} - 1 \right] - Q \tag{17}$$

and next, its zero is designated. As can be seen in Figure 2, the g(x) function has two zeros.
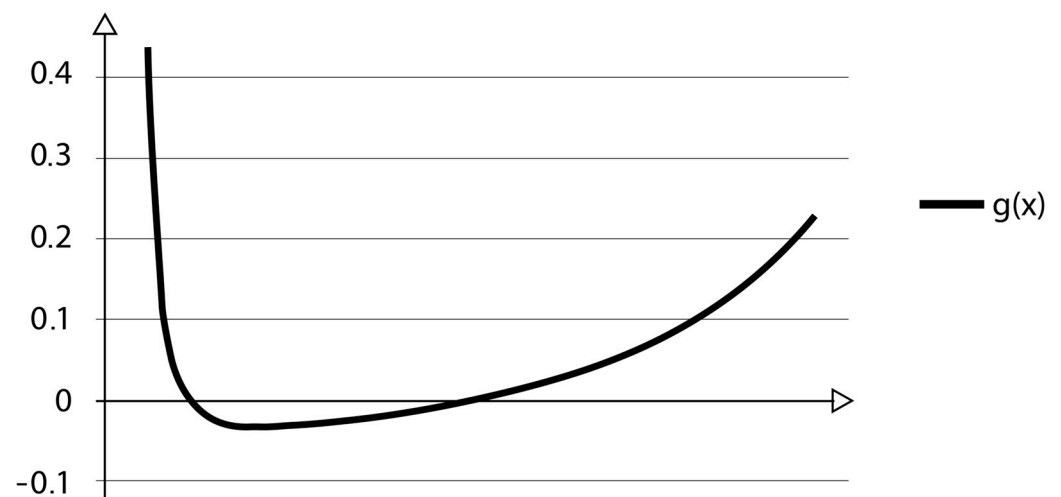

Figure 2. g(x) function graph.

The condition of physical interpretation of solving Equation (17) is the value of its zero, $\left(x = \frac{dp}{dl} \right)$, ensuring a positive shear rate value:

$$\left(-\frac{dv}{dr} \right) = G\sinh\left(\frac{r}{2D}\frac{dp}{dl} - \frac{\tau_y}{D} \right) > 0 \tag{18}$$

For G > 0, a physical condition is obtained, which has to meet the root of Equation (17):

$$x > \frac{2\tau_y}{R} \qquad (19)$$

It is proposed to solve the relationship g(x) = 0 by means of numerical methods: the bisection method, the Newton–Raphson method, the regula falsi method, combined methods, etc. [8–10]. To this end, the Department of Drilling and Geoengineering, at the Faculty of Drilling, Oil and Gas, AGH University of Science and Technology in Kraków, developed a numerical program, using the bisection method. The algorithm of solving numerical Equation (17) is presented in Figure 3.

The boundaries of the interval of the solution being sought $\left(x_{sr} = \frac{dp}{dl}\right)$ are suggested as follows: $a = \frac{2\tau_y}{R}$, $b = 10^6$, the accuracy of its estimation epsilon = 0.00001. Total pressure losses are determined from the relationship $(p = x_{sr} \cdot L)$.
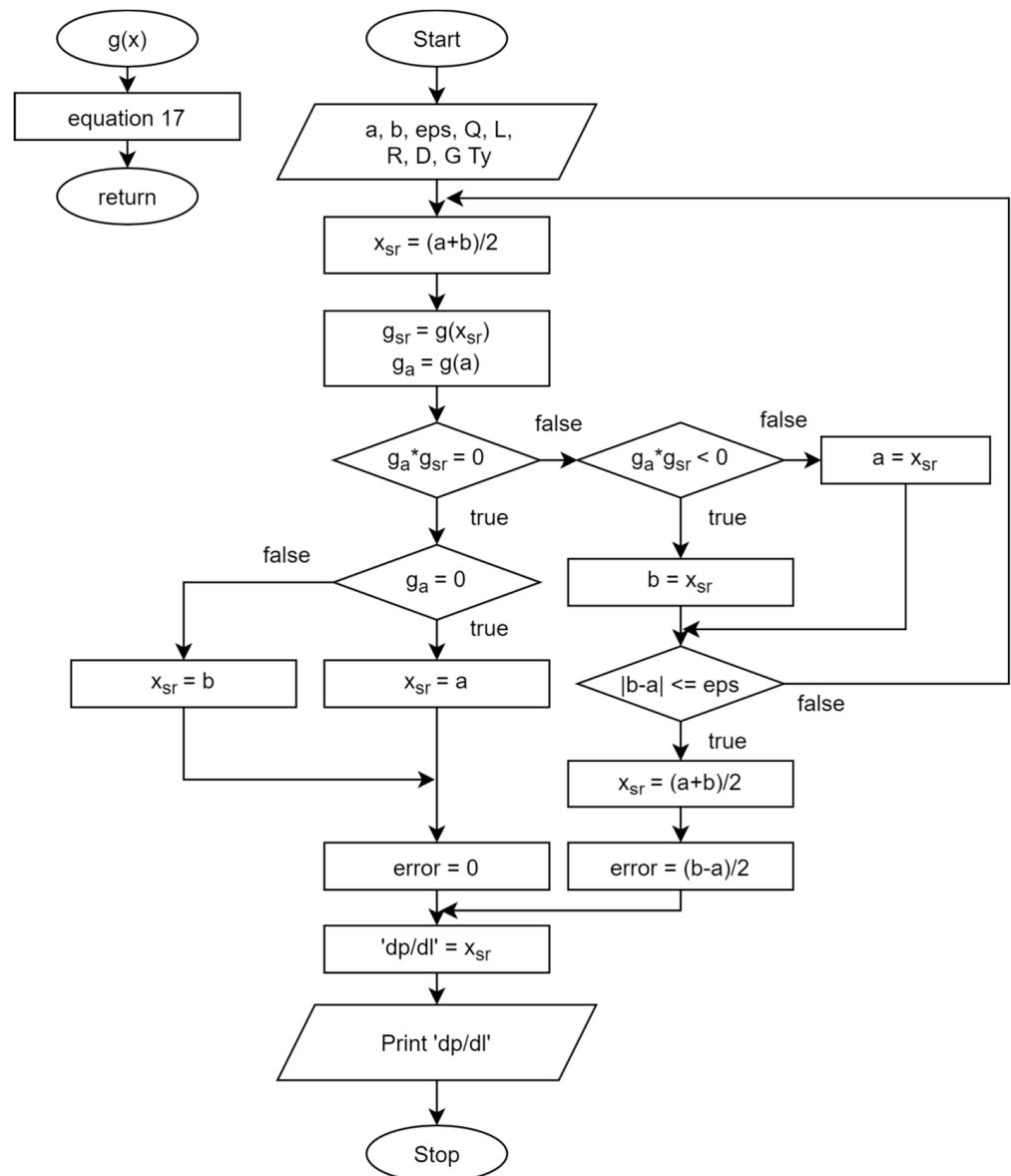

Figure 3. Block diagram for the calculation of root of the g(x) function being in the range [a, b] by means of the bisection method.

4. Determination of Rheological Parameters and Resistances of Drilling Fluid Laminar Flow

The selection of the accurate rheological model has an impact on the accuracy of the calculation results received. Drilling fluid rheological properties are measured by means of rotational viscometers of the following types: Fann, Chan, Brookfield, Haake, and Ofite [11–16]. A fluid test consists in determining shear stresses relationships (τ) in a shear rate function $\left(\dot{\gamma} = \left(-\frac{dv}{dr} \right) \right)$. Drilling fluid (Bingham, pseudoplastic and Herschel–Bulkley) the rheological parameters are specified on the basis of standards [3,4] and the relationships which are developed and not accounted for in the standards [6,17].

In order to determine rheological parameters for a three-parameter Vom Berg fluid model, it is necessary to know the shear stress values for three shear rates ($\dot{\gamma}_{LOW}$, $\dot{\gamma}_{MID}$, $\dot{\gamma}_{TOP}$).

The basic problem is to determine a real value of fluid shear rate ($\dot{\gamma}_{MID}$). Apart from its rheological parameters, also flow conditions, such as a stream of flow volume and geometry of an element in which flow takes place, have an impact on the real value of shear rates of flowing drilling fluid. Precise values of real shear rates of fluid can be determined from Formula (6) only after establishing fluid rheological parameters.

For the laminar flow of a Newtonian fluid through a pipe, the shear rate is determined as follows [18]:

$$\dot{\gamma} = \left(-\frac{dv}{dr} \right) = \frac{8v}{d} \tag{20}$$

This value is proposed to be assumed as the starting point for establishing the actual scope of shear rates for the Vom Berg fluid.

Therefore, it is suggested, before starting calculations, to determine the shear rate value ($\dot{\gamma}$) from Formula (20). Next, for a given viscometer, by means of which dependences between shear stresses and shear rate are determined, the most approximated value of $\dot{\gamma}_{MID} \approx \frac{8v}{d}$ should be adopted. The value will define the shear rate interval, which should be considered in calculations of drilling fluid rheological parameters $\dot{\gamma}_{MID} \in (\dot{\gamma}_{LOW} ; \dot{\gamma}_{TOP})$. The value $\dot{\gamma}_{LOW}$ is the closest shear rate value smaller than $\dot{\gamma}_{MID}$ recorded on a viscometer. The value $\dot{\gamma}_{TOP}$ is the closest shear rate value larger than $\dot{\gamma}_{MID}$ recorded on a viscometer. For the assumed shear rate values $\left(\dot{\gamma}_{LOW}, \dot{\gamma}_{MID}, \dot{\gamma}_{TOP} \right)$ and shear stresses corresponding to them ($\tau_{LOW}, \tau_{MID}, \tau_{TOP}$), one may determine rheological parameters of fluid (τ_y, D and G) described with the Vom Berg model.

For the Vom Berg fluid model, rheological parameters: τ_y, D and G are determined by solving the following system of equations:

$$\begin{cases} \tau_{TOP} = \tau_y + D \sinh^{-1}\left(\frac{\dot{\gamma}_{TOP}}{G} \right) \\ \tau_{MID} = \tau_y + D \sinh^{-1}\left(\frac{\dot{\gamma}_{MID}}{G} \right) \\ \tau_{LOW} = \tau_y + D \sinh^{-1}\left(\frac{\dot{\gamma}_{LOW}}{G} \right) \end{cases} \tag{21}$$

The value of the G parameter is obtained from the numerical solution of the equation:

$$\frac{\sinh^{-1}\left(\frac{\dot{\gamma}_{TOP}}{G} \right) - \sinh^{-1}\left(\frac{\dot{\gamma}_{MID}}{G} \right)}{\sinh^{-1}\left(\frac{\dot{\gamma}_{TOP}}{G} \right) - \sinh^{-1}\left(\frac{\dot{\gamma}_{LOW}}{G} \right)} = \frac{\tau_{TOP} - \tau_{MID}}{\tau_{TOP} - \tau_{LOW}} \tag{22}$$

In order to solve Equation (22), it is assumed that x = G and the g(x) function is created:

$$g(x) = \frac{\sinh^{-1}\left(\frac{\dot{\gamma}_{TOP}}{x} \right) - \sinh^{-1}\left(\frac{\dot{\gamma}_{MID}}{x} \right)}{\sinh^{-1}\left(\frac{\dot{\gamma}_{TOP}}{x} \right) - \sinh^{-1}\left(\frac{\dot{\gamma}_{LOW}}{x} \right)} - \frac{\tau_{TOP} - \tau_{MID}}{\tau_{TOP} - \tau_{LOW}} \tag{23}$$

and next its zero is designated.

The solution of the g(x) = 0 relationship is proposed by means of the numerical methods: the bisection method, the Newton–Raphson method, the regula falsi method, combined methods, etc. [8,9,19]. The algorithm of solving Equation (23) by means of the secant method is presented in Figure 4.
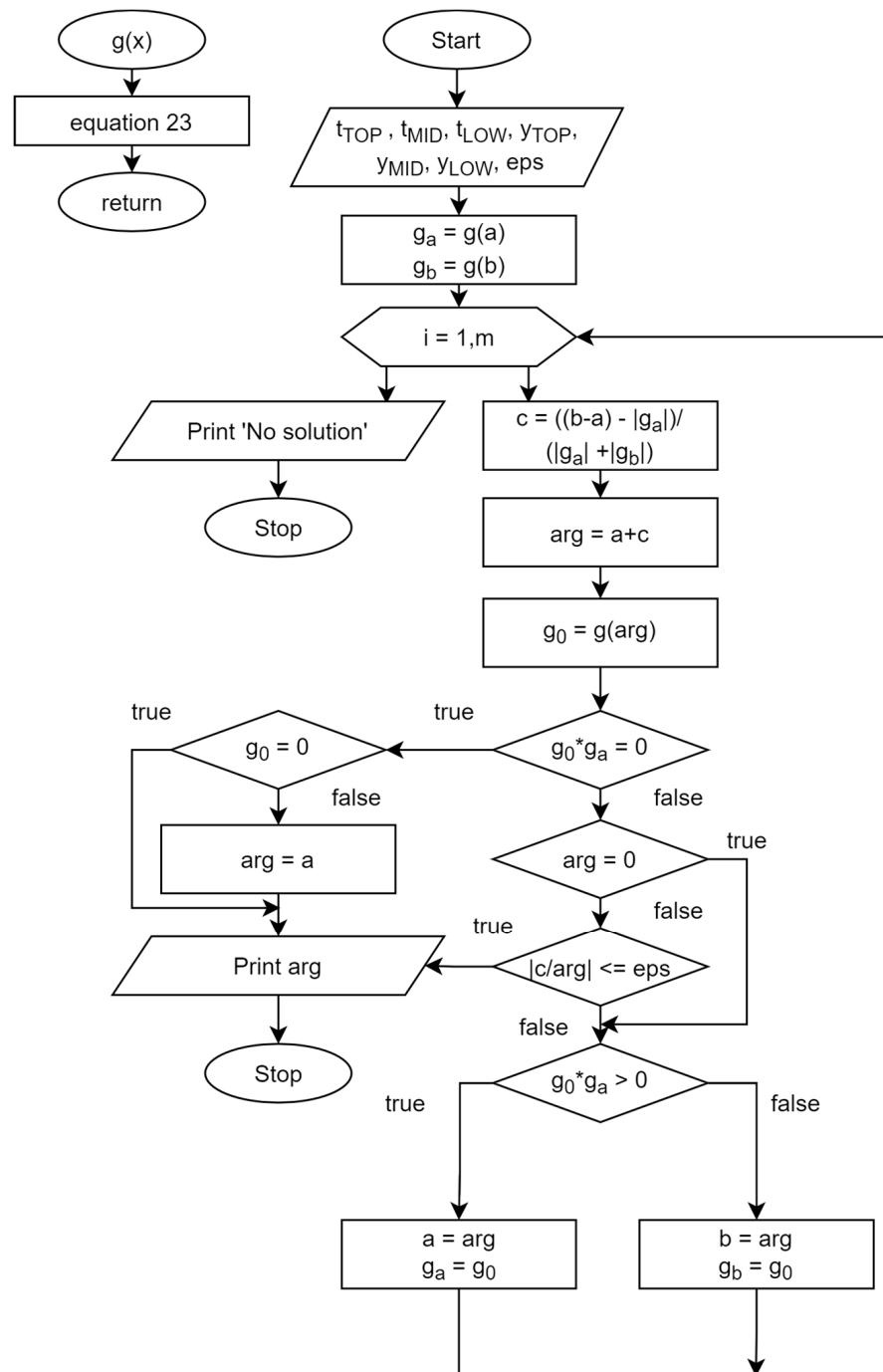

Figure 4. Block diagram for the calculation of the root of the g(x) function being in the range [a, b] by means of the secant method.

When analysing the existence of the solution of the Equation (23), we should analyse the g(x) function flow. Assuming:

$$g(x) = f(x) - W \qquad (24)$$

where:

$$f(x) = \frac{\sinh^{-1}\left(\frac{\dot{\gamma}_{TOP}}{x}\right) - \sinh^{-1}\left(\frac{\dot{\gamma}_{MID}}{x}\right)}{\sinh^{-1}\left(\frac{\dot{\gamma}_{TOP}}{x}\right) - \sinh^{-1}\left(\frac{\dot{\gamma}_{LOW}}{x}\right)}, \text{ and } W = \frac{\tau_{TOP} - \tau_{MID}}{\tau_{MID} - \tau_{LOW}}$$

one should state that the g(x) function is the f(x) function shifted in relation to the axis of dependent variables by the value W. Analysing the f(x) function flow for positive values x, it can be stated that it is a continuous, increasing and differentiable function. It also does not intersect the OX axis.

The smallest value is obtained for x→0: $f(x)_{MIN} = \lim\limits_{x \to 0} f(x)$.

Whereas the highest value is obtained for x→∞: $f(x)_{MAX} = \lim\limits_{x \to \infty} f(x)$.

The g(x) function will intersect the OX axis when $W \geq f(x)_{MIN}$ and when $W \leq f(x)_{MAX}$. Figure 5 shows the g(x) function flow depending on the W parameter value.
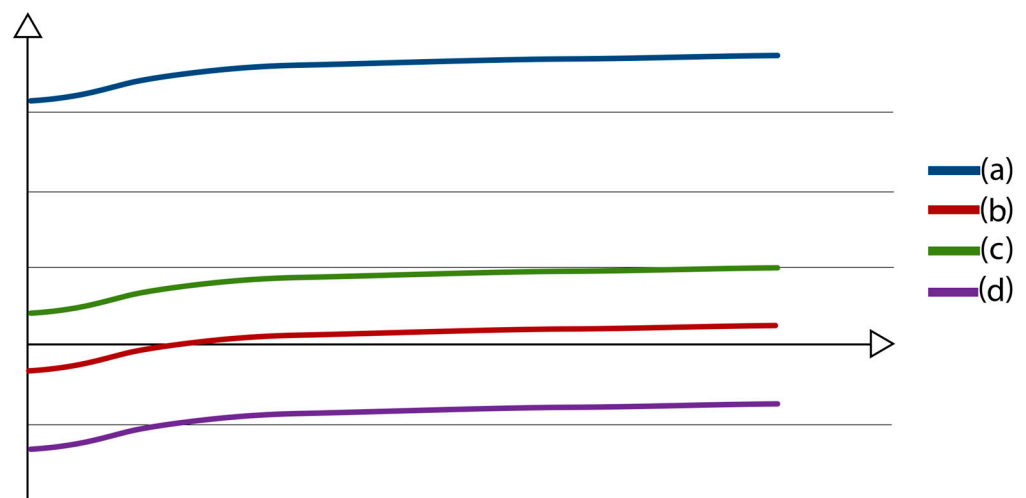

Figure 5. g(x) function flow depending on the W value: (**a**) W = 0, g(x) = f(x); (**b**) $f(x)_{MIN} < W < f(x)_{MAX}$; (**c**) $W < f(x)_{MIN}$; (**d**) $W > f(x)_{MAX}$.

The g(x) function will have a root when the following condition is met:

$$\lim\limits_{x \to 0} f(x) < \frac{\tau_{TOP} - \tau_{MID}}{\tau_{TOP} - \tau_{LOW}} < \lim\limits_{x \to \infty} f(x) \tag{25}$$

Taking into account

$$f(x)_{MIN} = \lim\limits_{x \to 0} f(x) = \lim\limits_{x \to 0} \frac{\sinh^{-1}\left(\frac{\dot{\gamma}_{TOP}}{x}\right) - \sinh^{-1}\left(\frac{\dot{\gamma}_{MID}}{x}\right)}{\sinh^{-1}\left(\frac{\dot{\gamma}_{TOP}}{x}\right) - \sinh^{-1}\left(\frac{\dot{\gamma}_{200}}{x}\right)} = \lim\limits_{x \to 0} \frac{\ln\left(\frac{\dot{\gamma}_{TOP} + \sqrt{(\dot{\gamma}_{TOP})^2 + x^2}}{\dot{\gamma}_{MID} + \sqrt{(\dot{\gamma}_{MID})^2 + x^2}}\right)}{\ln\left(\frac{\dot{\gamma}_{TOP} + \sqrt{(\dot{\gamma}_{TOP})^2 + x^2}}{\dot{\gamma}_{LOW} + \sqrt{(\dot{\gamma}_{LOW})^2 + x^2}}\right)} = \frac{\ln\left(\frac{\dot{\gamma}_{TOP}}{\dot{\gamma}_{MID}}\right)}{\ln\left(\frac{\dot{\gamma}_{TOP}}{\dot{\gamma}_{LOW}}\right)}$$

$$f(x)_{MAX} = \lim\limits_{x \to \infty} f(x) = \lim\limits_{x \to \infty} \frac{\ln\left(\frac{\dot{\gamma}_{TOP} + \sqrt{(\dot{\gamma}_{TOP})^2 + x^2}}{\dot{\gamma}_{MID} + \sqrt{(\dot{\gamma}_{MID})^2 + x^2}}\right)}{\ln\left(\frac{\dot{\gamma}_{TOP} + \sqrt{(\dot{\gamma}_{TOP})^2 + x^2}}{\dot{\gamma}_{LOW} + \sqrt{(\dot{\gamma}_{LOW})^2 + x^2}}\right)} = \lim\limits_{x \to \infty} \frac{\left(\ln\left(\frac{\dot{\gamma}_{TOP} + \sqrt{(\dot{\gamma}_{TOP})^2 + x^2}}{\dot{\gamma}_{MID} + \sqrt{(\dot{\gamma}_{MID})^2 + x^2}}\right)\right)'}{\left(\ln\left(\frac{\dot{\gamma}_{TOP} + \sqrt{(\dot{\gamma}_{TOP})^2 + x^2}}{\dot{\gamma}_{LOW} + \sqrt{(\dot{\gamma}_{LOW})^2 + x^2}}\right)\right)'}$$

$$= \lim\limits_{x \to \infty} \frac{\left(\frac{\dot{\gamma}_{LOW}}{x} + \sqrt{\left(\frac{\dot{\gamma}_{LOW}}{x}\right)^2 + 1}\right)}{\left(\frac{\dot{\gamma}_{MID}}{x} + \sqrt{\left(\frac{\dot{\gamma}_{MID}}{x}\right)^2 + 1}\right)} \cdot \frac{\left(\sqrt{\left(\frac{\dot{\gamma}_{LOW}}{x}\right)^2 + 1}\right)}{\left(\sqrt{\left(\frac{\dot{\gamma}_{MID}}{x}\right)^2 + 1}\right)}$$

$$\frac{\dot{\gamma}_{\text{TOP}}\left(\sqrt{\left(\frac{\dot{\gamma}_{\text{TOP}}}{x}\right)^2 + 1}\right) + \left(\frac{\dot{\gamma}_{\text{TOP}}}{x}\right)^2 - \dot{\gamma}_{\text{MID}}\left(\sqrt{\left(\frac{\dot{\gamma}_{\text{MID}}}{x}\right)^2 + 1}\right) - \left(\frac{\dot{\gamma}_{\text{MID}}}{x}\right)^2}{\dot{\gamma}_{\text{TOP}}\left(\sqrt{\left(\frac{\dot{\gamma}_{\text{TOP}}}{x}\right)^2 + 1}\right) + \left(\frac{\dot{\gamma}_{\text{TOP}}}{x}\right)^2 - \dot{\gamma}_{\text{LOW}}\left(\sqrt{\left(\frac{\dot{\gamma}_{\text{LOW}}}{x}\right)^2 + 1}\right) - \left(\frac{\dot{\gamma}_{\text{LOW}}}{x}\right)^2} = \frac{\dot{\gamma}_{\text{TOP}} - \dot{\gamma}_{\text{MID}}}{\dot{\gamma}_{\text{TOP}} - \dot{\gamma}_{\text{LOW}}}$$

the condition of occurrence of the root of the g(x) function is obtained:

$$\frac{\ln\left(\frac{\dot{\gamma}_{\text{TOP}}}{\dot{\gamma}_{\text{MID}}}\right)}{\ln\left(\frac{\dot{\gamma}_{\text{TOP}}}{\dot{\gamma}_{\text{LOW}}}\right)} < \frac{\tau_{\text{TOP}} - \tau_{\text{MID}}}{\tau_{\text{TOP}} - \tau_{\text{LOW}}} < \frac{\dot{\gamma}_{\text{TOP}} - \dot{\gamma}_{\text{MID}}}{\dot{\gamma}_{\text{TOP}} - \dot{\gamma}_{\text{LOW}}} \tag{26}$$

Knowing the value of the G parameter (G = x), the other rheological parameters should be determined from the following relationship:

$$D = \frac{\tau_{\text{TOP}} - \tau_{\text{MID}}}{\sinh^{-1}\left(\frac{\dot{\gamma}_{\text{TOP}}}{G}\right) - \sinh^{-1}\left(\frac{\dot{\gamma}_{\text{MID}}}{G}\right)} \tag{27}$$

$$\tau_y = \tau_{\text{TOP}} - D\sinh^{-1}\left(\frac{\dot{\gamma}_{\text{TOP}}}{G}\right) \tag{28}$$

The calculated rheological parameters of the Vom Berg model (τ_y, D and G) enable to determine unit flow resistances $\left(\frac{\text{dp}}{\text{dl}}\right)$ of a fluid stream (Q) flowing inside a pipe with the radius (R).

The following algorithm is suggested:

1. Measurement, by means of a viscometer, shear stress dependencies for different drilling fluid shear rate values.
2. Estimation of the approximated shear rate value ($\dot{\gamma}_{\text{START}}$) (occurring when fluid stream (Q) flows inside a pipe with the radius (R). Formula (20).
3. Determination of the most approximated shear rate value ($\dot{\gamma}_{\text{MID}} \approx \dot{\gamma}_{\text{START}}$), taking into account shear stress dependencies on shear rate, obtained from a given viscometer; establishment of the value ($\dot{\gamma}_{\text{LOW}}, \dot{\gamma}_{\text{TOP}}$). Determination of the measured values ($\tau_{\text{LOW}}, \tau_{\text{MID}}, \tau_{\text{TOP}}$).
4. Calculation of rheological parameters of the fluid described by the Vom Berg model. Numerical solution of the Equation (22) and use of relationships (27) and (28).
5. Calculation of unit flow resistances $\left(\frac{\text{dp}}{\text{dl}}\right)$. Numerical solution of Equation (17).
6. Calculation of real shear rate ($\dot{\gamma}_{\text{START}}$), characterising fluid flow, Equation (8).
7. Evaluation of the accuracy of the assumptions made in Item 3 of the algorithm. Checking of the condition $\dot{\gamma}_{\text{START}} \in (\dot{\gamma}_{\text{LOW}}, \dot{\gamma}_{\text{TOP}})$. If this condition is met, calculations of unit flow resistances are considered completed.

If the condition $\dot{\gamma}_{\text{START}} \in (\dot{\gamma}_{\text{LOW}}, \dot{\gamma}_{\text{TOP}})$ is not met, calculations are repeated beginning with Item 3, assuming the value of the real shear rate ($\dot{\gamma}_{\text{START}}$) determined in Item 6.

5. Application of Derived Equations in Cloud-Hosted Computer-Aided Design (CAD) Tool

The main purpose of the presented work was to derive and present mathematical formulas of laminar flow of the Vom Berg model. In order to present the formulas application possibilities to larger audience, the authors created a new computer-aided design tool. The tool is called the HDD Designer, and it is available on the Internet via web browsers. The address of the tools is www.HDDDesigner.com, accessed on 10 June 2022.

Rheology Sim is the first finished module in the HDD Designer, and it includes following features:

- Rheological parameters calculation.

- Rheological model specific parameters calculation for Newton, Bingham, Casson, Ostwald De Waele, Herschel–Bulkley, Vom Berg and Eyring models.
- Regression parameters calculation.
- Graphical and tabular result presentation.

As the next step, the authors plan to develop another module for calculations of flow resistances and pressure losses during laminar flow of fluid in a drill pipe and annulus for various rheological models.

The graphical user interface of the tool is presented on the Figure 6. The HDD Designer has been built with use of Angular (Graphical User Interface) and NET Core (application programming interface), it is hosted on Microsoft Azure Cloud. As it uses the most recent available technologies and cloud hosting, it is an easily expandable, robust, scalable and high availability application.
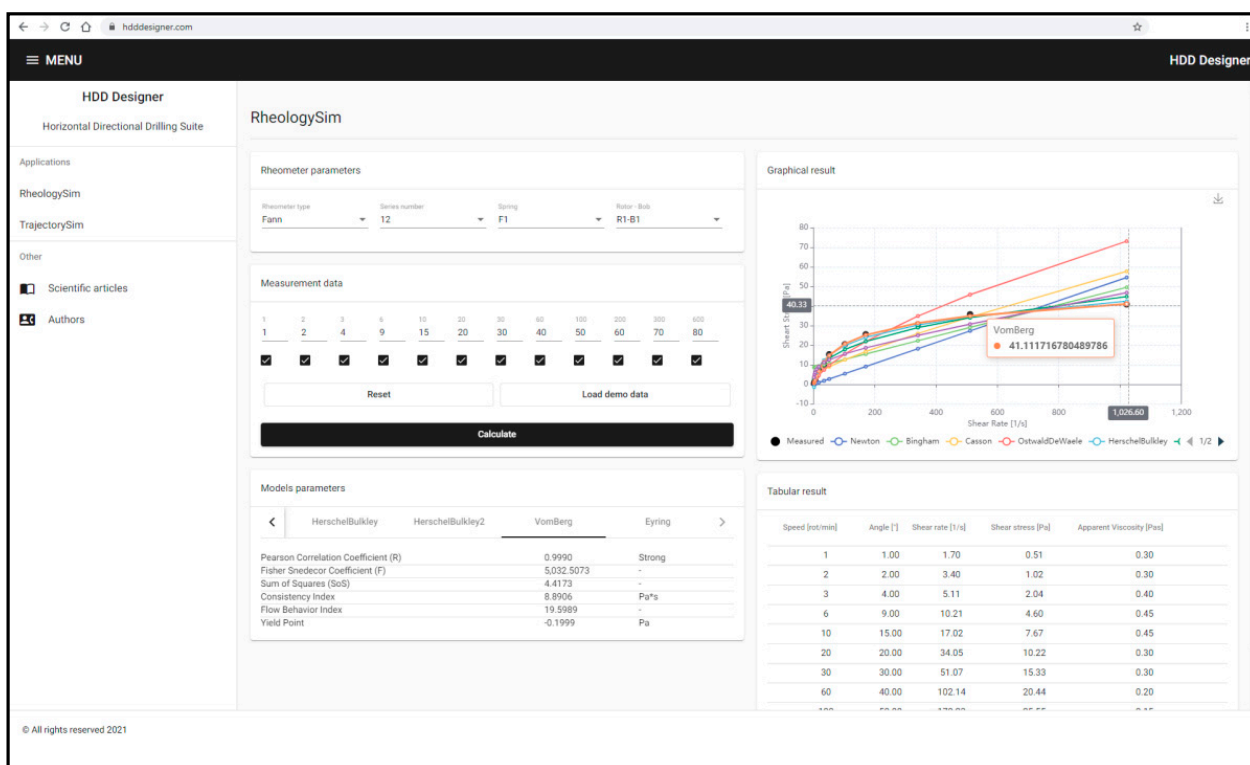

Figure 6. Graphical user interface (GUI) of the HDD Designer. The HDD Designer is available on www.hdddesigner.com (accessed on 10 June 2022).

6. A practical Example of the Proposed Methodology Application

The Vom Berg model can be applied to various technological fluids, such as drilling muds, drill-in fluids, fracturing fluids, spacers, washes and cement slurries. In order to apply the Vom Berg model in practice, the unit flow resistances $\left(\frac{dp}{dl}\right)$ were calculated for the selected sealing slurry.

In order to exemplify the developed relationships, flow resistances of cement slurry pumped to casing with the external diameter of $6\,{}^5/_8{}''$ (the radius of the pipe interior R = 0.0736 m), with a stream of flow volume Q = 0.03 m^3/s were calculated.

By means of a Fann 35 rotational viscometer (in the arrangement R1-B1 and a spring F1), rheological properties of cement slurry to be used in a borehole [15] were measured. The measurement results of a torsion angle of the outer cylinder (Φ), read for the specified rotational speeds (n) and calculated shear stress values (τ) and shear rate ($\dot{\gamma}$), occurring during measurements, are provided in Table 1. A graphical comparison of popular rheological models' fitness to measured values is presented on Figure 7. Table 2 shows the

tabular comparisons of statistical parameters from popular rheological models. Based on both comparisons it is visible that the Vom Berg model achieved the highest fitness for the analysed example.

Next, on the basis of the developed methodology, the slurry rheological parameters and unit flow resistances were calculated, assuming the Vom Berg fluid model.

To this end, the approximated shear rate inside $6\,^5/_8''$ casing ($\dot{\gamma}_{START} \approx 96\,\mathrm{s}^{-1}$) was estimated, using Equation (18). That value was used for estimating the value of $\dot{\gamma}_{LOW}$, $\dot{\gamma}_{MID}$ and $\dot{\gamma}_{TOP}$. For those values, the slurry rheological parameters and unit flow resistances were calculated. The calculation of real shear rate $\dot{\gamma}_{START} = 101.6\,\mathrm{s}^{-1}$ and comparing it with its acceptable range $\dot{\gamma}_{START} \in (\dot{\gamma}_{LOW}, \dot{\gamma}_{TOP})$ confirmed the accuracy of the assumptions made. The calculation results are spresented in Table 3.

Table 1. Results of laboratory measurements and calculations of shear stresses and shear rates for cement slurry tested on a 12 speed Fann viscometer 35A/SR-12, with the arrangement of cylinders R1-B1 and spring F1 [15].

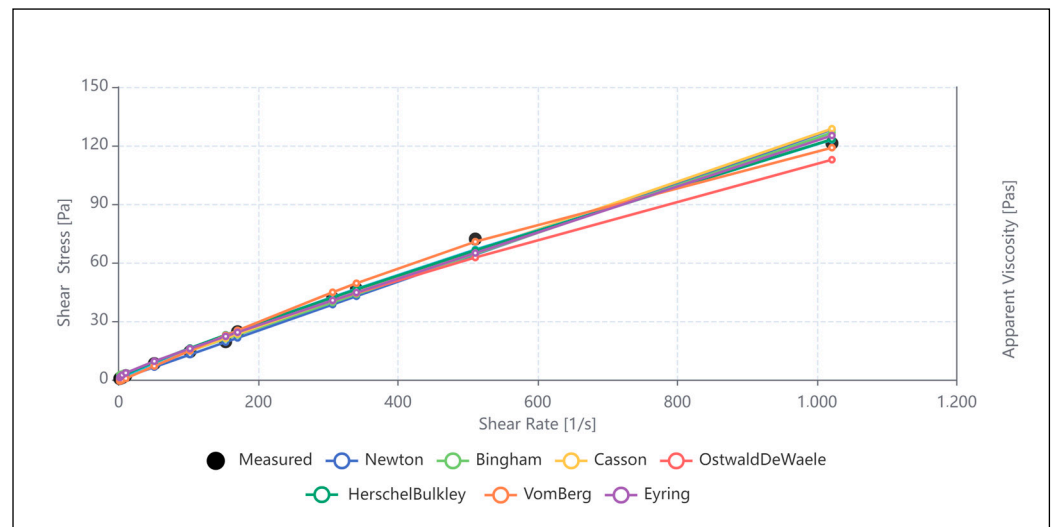| Laboratory Measurement												
Rotational speed n, [rot/min]	0.9	1.8	3	6	30	60	90	100	180	200	300	600
Torsion	1	2	2	4	16	28	38	48	82	91	141	237
Angle Φ, [-]												
Calculated Values												
Shear rate $\dot{\gamma}$, [s^{-1}]	1.53	3.07	5.11	10.22	51.10	102.20	153.31	170.34	306.61	340.68	511.02	1022.04
Shear stresses τ, [Pa]	0.51	1.02	1.02	2.04	8.18	14.31	19.42	24.53	41.90	46.50	72.05	121.11

Figure 7. Graphical comparison of rheological models' fitness to the measurement.

Table 2. Tabular comparison of rheological models' fitness to the measurement.

Model	Newton	Bingham	Casson	Ostwal De Waele	Herschel Bulkley	Eyring	Vom Berg
Pearson Correlation Coefficient	0.9947	0.996	0.9965	0.9939	0.998	0.997	0.9985
Fisher Snedecor Coefficient	929.58	1230.19	1425.92	805.64	2556.01	1649.97	3379.23
Sum of squares	156.17	118.31	102.19	179.9	57.18	88.39	43.29

Table 3. Results of calculations with regard to rheological parameters of the tested cement slurry.

Approximated shear rate $\dot{\gamma}_{\mathbf{START}}$, [s^{-1}]	96		
Shear rate $\dot{\gamma}$, [s^{-1}]	$\dot{\gamma}_{LOW} = \dot{\gamma}_{30}$ 51.10	$\dot{\gamma}_{MID} = \dot{\gamma}_{60}$ 102.20	$\dot{\gamma}_{TOP} = \dot{\gamma}_{90}$ 153.31
Shear stresses τ, [Pa]	$\tau_{LOW} = \tau_{30}$ 8.18	$\tau_{MID} = \tau_{60}$ 14.31	$\tau_{TOP} = \tau_{90}$ 19.42
Rheological parameters of the Vom Berg model	τy 1.2448	D 18.3547	G 132.16
Unit flow resistances dp/dl [Pa/m]	387		
Real shear rate $\dot{\gamma}_{\mathbf{START}}$, [s^{-1}] $\dot{\gamma}_{\mathbf{START}} \in (\dot{\gamma}_{\mathbf{LOW}}, \dot{\gamma}_{\mathbf{TOP}})$	101.6		

7. Conclusions

In the case of fluids that demonstrate features of both viscoelastic and pseudoplastic fluids, we should consider other rheological models than those used so far in the drilling industry. One of the possible models to be applied is the Vom Berg model.

When describing the laminar flow of Vom Berg fluids through a pipe, we should use the relationships introduced in this article. The above-presented limitations and conditions of obtaining an unambiguous solution of Equation (17) allow for numerical calculation of resistances of the laminar flow of Vom Berg fluids. The proposed block diagram and the developed HDD Designer application should be used in engineering practice.

Rheological parameters of the Vom Berg model should be determined depending on the real shear rate, recorded during drilling fluid flow. To this end, the methodology suggested in this article should be applied.

Author Contributions: Conceptualisation, R.W. and G.O.; Data curation, R.W. and G.O.; Formal analysis, R.W. and G.O.; Funding acquisition, R.W.; Investigation, R.W. and G.O.; Methodology, R.W. and G.O.; Project administration, R.W.; Resources, R.W.; Software, G.O.; Supervision, R.W.; Validation, R.W. and G.O.; Visualisation, R.W. and G.O.; Writing—original draft, R.W. and G.O.; Writing—review and editing, G.O. All authors have read and agreed to the published version of the manuscript.

Institutional Review Board Statement: Not applicable.

Informed Consent Statement: Not applicable.

Data Availability Statement: Not applicable.

Nomenclature

a, b	interval boundaries in the bisection method or the regula falsi method, [-];
C_1	constant;
d	internal pipe diameter, [m];
D	rheological parameter in the Vom Berg model, [Pa];
η	plastic viscosity, [Pas];
G	rheological parameter in the Vom Berg model, [s^{-1}];
$\dot{\gamma}$	shear rate gradient, [s^{-1}];
$\dot{\gamma}_{LOW}$	lower measured value of a shear rate gradient, [s^{-1}];
$\dot{\gamma}_{MID}$	middle measured value of a shear rate gradient, [s^{-1}];
$\dot{\gamma}_{START}$	reference shear rate gradient, [s^{-1}];
$\dot{\gamma}_{TOP}$	upper measured value of a shear rate gradient, [s^{-1}];

k	coefficient of drilling fluid consistency, [Pas^n];
n	exponential index, [-];
p	pressure, [Pa];
Q	flow rate, [m^3/s];
R	internal radius, [m];
r	distance from the pipe axis, [m];
r_0	distance from the axis of a pipe in which fluid flows with constant velocity v_0, [m];
τ	shear stress, [Pa];
τ_y	yield point, [Pa];
τ_{LOW}	lower measured value of shear stress, [Pa];
τ_{MID}	middle measured value of shear stress, [Pa];
τ_{TOP}	upper measured value of shear stress, [Pa];
v	flow velocity, [m/s];
v_{max}	maximum flow velocity, [m/s];
v_0	constant fluid flow velocity at a distance from 0 to r_0 from the pipe axis, [m/s];

References

1. Vom Berg, W. Influence of specific surface and concentration of solids upon the fow behaviour of cement pastes. *Mag. Concr. Res.* **1979**, *31*, 211–216. [CrossRef]
2. Wiśniowski, R.; Skrzypaszek, K.; Małachowski, T. Selection of a Suitable Rheological Model for Drilling Fluid Using Applied Numerical Methods. *Energies* **2020**, *13*, 3192. [CrossRef]
3. API RP 13D. *Rheology and Hydraulics of Oil-Well Drilling Fluids*; Norm of American Petroleum Institute: Washington, DC, USA, 2006.
4. *BN-90/1785-01*; Płuczka Wiertnicza. Metody Badań w Warunkach Polowych. Wydawnictwa Normalizacjne "ALFA": Warszawa, Poland, 1990.
5. Wiśniowski, R. *Metodyka Określania Modelu Reologicznego Cieczy Wiertniczej*; Wiertnictwo, Nafta, Gaz R. 18/1; Wydawnictwo AGH: Kraków, Poland, 2001.
6. Wiśniowski, R. *Zastosowanie Modelu Herschela-Bulkleya w Hydraulice Płuczek Wiertniczych*; Nowoczesne Techniki i Technologie Bezwykopowe, Zeszyt nr 2/2000; HDD Consulting: Kraków, Poland, 2000; pp. 20–28.
7. Benyounes, K. Rheological behavior of cement-based grout with Algerian bentonite. *SN Appl. Sci.* **2019**, *1*, 1037. [CrossRef]
8. Ahmad, A.G. Comparative Study of Bisection and Newton-Rhapson Methods of Root-Finding Problems. *Int. J. Math. Trends Technol. (IJMTT)* **2015**, *V19*, 121–129. [CrossRef]
9. Dalquist, G.; Biorck, A. *Numerical Methods*; Dower Publication Inc.: Mineula, NY, USA, 2003.
10. Ehiwario, J.C.; Aghamie, S.O. Comparative Study of Bisection, Newton-Raphson and Secant Methods of Root-Finding Problems. *IOSR J. Eng. (IOSRJEN)* **2014**, *4*, 1–7.
11. Catalogue of Brookfield Company. *Brookfield Viscometers/Rheometers*; Catalogue of Brookfield Company: Middleboro, MA, USA, 1999.
12. Thermo Fisher Scientific Inc. *Haake Series 1*; Materials from Thermo Fisher Scientific; Thermo Fisher Scientific Inc.: Hanover, Germany, 2018.
13. Materials of Rheology Solution Victoria Company. *Haake, Material Characterisation & Testing Products*; Materials of Rheology Solution Victoria Company: Truganina, Australia, 2019.
14. Hoechst. *Hoechst Polymer Fluids*; Information Materials from Hoechst; Hoechst: Höchst, Germany, 1989.
15. Fann Instrument Company. *Model 35 Instruction Manual, Manual No. 208878*; Fann Instrument Company: Houston, TX, USA, 2016.
16. OFI Testing Equipment, Inc. Testing Equipment for Drilling Fluids · Cement · Core Analysis · Laboratory Supplies · Reagents, Ofite Catalog. 2017. Available online: https://hiltoninstruments.com/pdfUploads/OFITE%20Catalogue.pdf (accessed on 10 June 2022).
17. Klotz, J.A.; Brigham, W.E. To Determine Herschel-Bulkley Coefficients. *J. Pet. Technol.* **1998**, *50*, 80–81. [CrossRef]
18. Bourgoyne, A.T.; Milheim, K.K.; Chenevert, M.E.; Young, F.S. Applied Drilling Engineering. In *SPE Textbook*; SPE: Houston, TX, USA, 1986; Chapter 4.8.
19. Chen, J.; Li, W. An improved exponential regula falsi method with quadratic convergence of both diameter and point for solving nonlinear equations. *Appl. Numer. Math.* **2007**, *57*, 80–88. [CrossRef]